Research Square

Preprints are preliminary reports that have not undergone peer review.
They should not be considered conclusive, used to inform clinical practice,
or referenced by the media as validated information.

Visible-Light-Driven Photocatalytic Degradation of Methylene Blue Using a Graphene Oxide/Sulfur Carbon Nitride (GO/SCN) Nanocomposite

Martin Ouma Osemba

mouma@associates.mku.ac.ke

Mount Kenya University https://orcid.org/0009-0007-2045-4746

Adrián Chávez Huerta

2. Zulian Institute of Technological Research (INZIT), Venezuela

Research Article

Keywords: Graphene oxide, Sulfur carbon nitride, Nanocomposite photocatalyst, Visible-light photocatalysis, Methylene blue degradation

Posted Date: March 25th, 2026

DOI: https://doi.org/10.21203/rs.3.rs-9207538/v1

License: This work is licensed under a Creative Commons Attribution 4.0 International License. Read Full License

Additional Declarations: The authors declare no competing interests.

Abstract

The development of efficient visible-light-responsive photocatalysts for the removal of persistent organic pollutants from wastewater remains an important challenge in environmental remediation. In this study, a graphene oxide/sulfur carbon nitride (GO/SCN) nanocomposite was synthesized and evaluated for the photocatalytic degradation of methylene blue (MB) under visible-light irradiation. Structural, morphological, and optical properties of the synthesized materials were characterized using X-ray diffraction (XRD), Fourier transform infrared spectroscopy (FTIR), scanning electron microscopy (SEM), ultraviolet–visible diffuse reflectance spectroscopy (UV–Vis DRS), and Brunauer–Emmett–Teller (BET) surface area analysis. XRD results confirmed the preservation of the graphitic carbon nitride structure with slight peak broadening after GO incorporation, while FTIR spectra indicated the presence of characteristic C–N heterocyclic vibrations and oxygen-containing functional groups from graphene oxide. SEM analysis revealed a layered and interconnected morphology with well-dispersed GO sheets within the SCN matrix. UV–Vis DRS analysis showed enhanced visible-light absorption with a red shift of the absorption edge from approximately 455 nm for pristine SCN to 475 nm for the GO/SCN composite. The optical band gap decreased from 2.72 eV for SCN to 2.58 eV for GO/SCN, indicating improved visible-light utilization. BET analysis demonstrated an increase in specific surface area from 32.6 $m^2 g^{-1}$ for SCN to 68.9 $m^2 g^{-1}$ for the GO/SCN nanocomposite, providing additional active sites for photocatalytic reactions. Photocatalytic experiments revealed that the GO/SCN nanocomposite achieved 96.4% degradation of methylene blue within 100 min under visible-light irradiation, significantly outperforming pristine SCN. Kinetic analysis showed that the degradation process followed pseudo-first-order reaction kinetics with an apparent rate constant of 0.032 min^{-1}. Radical scavenger experiments indicated that superoxide radicals ($\bullet O_2^-$), hydroxyl radicals (•OH), and photogenerated holes were the primary reactive species responsible for dye degradation. Furthermore, the photocatalyst exhibited excellent stability, maintaining over 90% degradation efficiency after five consecutive cycles. The enhanced photocatalytic performance is attributed to the synergistic interaction between graphene oxide and sulfur carbon nitride, which promotes efficient charge separation, improved electron transport, and increased adsorption of dye molecules. These findings demonstrate that GO/SCN nanocomposites represent promising metal-free photocatalysts for sustainable wastewater treatment and environmental purification applications.

1. Introduction

The rapid growth of industrialization and urbanization has significantly increased the discharge of organic pollutants into aquatic environments (MARTIN OUMA Osemba 2019). Among these pollutants, synthetic dyes released from textile, printing, paper, leather, and pharmaceutical industries represent a major environmental concern (Kallawar and Bhanvase 2023) due to their high chemical stability, toxicity, and resistance to natural biodegradation (Maghanga, Osemba, and Ojwang n.d.). These compounds can reduce light penetration in water bodies, disrupt aquatic ecosystems, and pose serious health risks to humans and wildlife (Mousavi et al. 2024). Methylene blue (MB), a widely used cationic dye in textile and medical industries, is frequently employed as a model organic pollutant for evaluating the efficiency of photocatalytic materials(Karthik et al. 2024) because of its well-defined optical properties and high stability in aqueous environments (Khan et al. 2023). Conventional wastewater treatment techniques such as adsorption, coagulation, chemical oxidation, and biological degradation have been widely used for dye removal (Kumari et al. 2024). However, these approaches often suffer from several limitations, including incomplete mineralization of pollutants, high operational costs, and the generation of secondary waste products (Ameen et al. 2025). In recent years, semiconductor-based photocatalysis has emerged as a promising advanced oxidation technology for environmental remediation (M. Osemba, Maghanga, and Ojwang 2025). Photocatalytic processes utilize light energy to generate highly reactive species such as hydroxyl radicals (•OH) and superoxide radicals ($\bullet O_2^-$), which can effectively degrade organic contaminants into harmless end products such as carbon dioxide and water (Ayu et al. 2023). Nevertheless, many conventional photocatalysts exhibit limited activity under visible light and suffer from rapid recombination of photogenerated electron–hole pairs, which significantly reduces their photocatalytic efficiency (Veedu et al. 2021). Graphitic carbon nitride ($g\text{-}C_3N_4$) and its modified derivatives have attracted considerable attention as metal-free photocatalysts due to their suitable band gap (~ 2.7 eV), good chemical stability, low toxicity, and ability to absorb visible light (Ahmed and Nishina 2026). Among the various modifications, sulfur-doped carbon nitride (SCN) has been reported to exhibit improved photocatalytic performance compared to pristine carbon nitride (Dhayal et al. 2026). Sulfur incorporation can modify the electronic structure of carbon nitride, narrow its band gap, enhance visible-light absorption, and improve the mobility of photogenerated charge carriers (Xie et al. 2025). Despite these advantages, the photocatalytic efficiency of SCN is still restricted by the relatively high recombination rate of photogenerated electron–hole pairs and limited surface adsorption sites (Eswaran et al. 2025). To overcome these limitations, the construction of heterostructured photocatalytic systems has become an effective strategy for improving charge separation and enhancing photocatalytic activity (J. Zhang et al. 2025). Graphene oxide (GO), a two-dimensional carbon-based nanomaterial rich in oxygen-containing functional groups, has been widely investigated as a promising support material in photocatalytic composites (M. O. Osemba et al. 2024). GO possesses

a large specific surface area, excellent electrical conductivity, and strong adsorption capability toward organic pollutants through π–π interactions (F. Zhang et al. 2024). When coupled with semiconductor photocatalysts, graphene oxide can act as an efficient electron acceptor and transport pathway, facilitating the separation of photogenerated charge carriers and suppressing their recombination (Al-Wasidi et al. 2025). The integration of graphene oxide with carbon nitride-based photocatalysts has therefore attracted significant interest for developing highly efficient visible-light photocatalytic systems. In such composites, graphene oxide not only enhances electron mobility but also improves surface adsorption of dye molecules and increases the number of active sites for photocatalytic reactions (Mutuku et al. 2025). These synergistic effects can significantly enhance the generation of reactive oxygen species responsible for pollutant degradation (Misra et al. 2023). In this study, a graphene oxide/sulfur carbon nitride (GO/SCN) nanocomposite was synthesized and evaluated as an efficient visible-light-responsive photocatalyst for the degradation of methylene blue in aqueous solution. The structural, morphological, and optical properties of the synthesized materials were characterized using various physicochemical techniques. The photocatalytic performance of the GO/SCN nanocomposite was investigated under visible-light irradiation, and the degradation kinetics of methylene blue were analyzed using a pseudo-first-order kinetic model. In addition, the possible photocatalytic mechanism responsible for the enhanced activity of the composite material was proposed. The findings of this study provide valuable insights into the design of graphene-based heterostructured photocatalysts for sustainable wastewater treatment and environmental remediation.

2. Materials and Methods

2.1 Materials

All chemicals used in this study were of analytical grade and were used without further purification. Graphene oxide (GO) powder, sulfur carbon nitride (SCN) precursors, and methylene blue (MB) dye were purchased from commercial suppliers. Ethanol and deionized water were used for all washing and solution preparation. Deionized water with a resistivity of 18.2 MΩ·cm was employed throughout all experiments.

2.2 Synthesis of GO/SCN Nanocomposite

The GO/SCN nanocomposite was synthesized through a controlled composite formation process to ensure uniform dispersion of graphene oxide sheets within the SCN matrix. Specifically, 50 mg of graphene oxide was dispersed in 50 mL of deionized water and ultrasonicated for 60 minutes to obtain a homogeneous suspension. Subsequently, 200 mg of SCN precursor was gradually added to the GO suspension under continuous magnetic stirring at 300 rpm. The mixture was stirred for an additional 2 hours at room temperature to facilitate thorough mixing and intimate contact between GO and SCN. The resulting mixture was then transferred to a ceramic crucible and subjected to thermal treatment at 550°C for 2 hours in air to promote the formation of the GO/SCN nanocomposite. After cooling to room temperature, the material was collected, washed repeatedly with deionized water and ethanol to remove residual precursors and impurities, and dried at 60°C for 12 hours to obtain a fine, stable powder.

2.3 Characterization of Materials

The physicochemical properties of GO, SCN, and the GO/SCN nanocomposite were evaluated using the following analytical techniques: X-ray Diffraction (XRD): The crystalline structure and phase composition were analyzed using a Cu Kα radiation source (λ = 1.5406 Å) over a 2θ range of 5–80°. Characteristic diffraction peaks corresponding to the (002) plane of SCN and the broad GO feature at lower angles were identified. Fourier Transform Infrared Spectroscopy (FTIR): FTIR spectra were recorded in the range of 400–4000 cm^{-1} to identify functional groups and confirm chemical interactions between SCN and GO. Scanning Electron Microscopy (SEM): Morphological and structural features were examined using SEM, revealing the layered SCN morphology and the dispersion of GO sheets within the composite matrix. UV–Visible Diffuse Reflectance Spectroscopy (UV–Vis DRS): Optical absorption and band gap properties were determined using UV–Vis DRS in the 200–800 nm range. Band gaps were estimated from Tauc plots assuming indirect allowed transitions. Brunauer–Emmett–Teller (BET) Surface Area Analysis: Nitrogen adsorption–desorption isotherms were measured at 77 K to calculate the specific surface area, pore volume, and average pore diameter.

2.4 Photocatalytic Activity Evaluation

The photocatalytic performance of the GO/SCN nanocomposite was evaluated via the degradation of methylene blue (MB) under visible-light irradiation. A 300 W Xe lamp equipped with a visible-light filter (λ > 420 nm) was used as the light source.

In a typical experiment, 50 mg of the photocatalyst was dispersed in 100 mL of MB aqueous solution with a concentration of 10 mg L^{-1}. The suspension was magnetically stirred in the dark for 30 minutes to allow adsorption–desorption equilibrium of MB onto the catalyst

surface. After equilibrium, the solution was irradiated with visible light while stirring to maintain uniform dispersion of the catalyst.

At predetermined intervals, 5 mL aliquots were withdrawn, centrifuged at 8000 rpm for 5 minutes to remove the catalyst, and the concentration of MB was determined by measuring the absorbance at 664 nm using a UV–Vis spectrophotometer. The photocatalytic degradation efficiency was calculated using:

$$\text{Degradation}:(\%) = \frac{C_0 - C_t}{C_0} \times 100 \quad \text{.....Eq. 1}$$

where $C_0$is the initial MB concentration and $C_t$is the concentration at time t.

2.5 Kinetic Analysis

The photocatalytic degradation kinetics of MB were analyzed using a pseudo-first-order model:

$$\ln\left(\frac{C_0}{C_t}\right) = kt \quad \text{.....Eq. 2}$$

where $k$is the apparent reaction rate constant (min^{-1}) and $t$is the irradiation time in minutes. The rate constant $k$was obtained from the slope of the linear plot of $\ln(C_0/C_t)$versus time.

2.6 Radical Scavenger Experiments

To identify the dominant reactive species involved in MB degradation, specific scavengers were added to the reaction system at a concentration of 1 mM before irradiation: Isopropanol (IPA) for hydroxyl radicals (•OH), Benzoquinone (BQ) for superoxide radicals ($•O_2^-$), and Ethylenediaminetetraacetic acid (EDTA) for photogenerated holes (h^+). The photocatalytic degradation efficiency was compared with control experiments to determine the contribution of each reactive species.

2.7 Catalyst Reusability and Stability

The stability and reusability of the GO/SCN nanocomposite were evaluated over five consecutive photocatalytic cycles. After each cycle, the catalyst was recovered by centrifugation, washed with deionized water and ethanol, and dried at 60°C for 6 hours before reuse. The structural integrity of the catalyst after the fifth cycle was confirmed using XRD, and the photocatalytic performance was compared to that of the fresh catalyst.

3. Results and Discussion

3.1 X-ray Diffraction (XRD) Analysis

The crystalline structure and phase composition of GO, SCN, and the GO/SCN nanocomposite were investigated using XRD as shown in Fig. 1 below.

The diffraction pattern of pristine SCN exhibited two characteristic peaks: a prominent peak at ~ 27° corresponding to the interlayer stacking of conjugated aromatic systems within the graphitic carbon nitride framework (002 plane), and a weaker peak at ~ 13°, attributed to in-plane structural packing of tri-s-triazine units. For GO, a broad peak at ~ 10° was observed, indicative of the layered structure and oxygenated functional groups present in graphene oxide sheets. In the GO/SCN nanocomposite, the characteristic SCN peaks were retained, demonstrating that the crystal structure of SCN remained largely intact after composite formation. A slight decrease in peak intensity and minor broadening suggested successful incorporation of GO into the SCN matrix, with strong interfacial interactions. No additional peaks were observed, confirming that no secondary phases or impurities formed during synthesis. The XRD results indicate that the heterostructured GO/SCN nanocomposite maintains the crystalline integrity of SCN while introducing GO layers that may facilitate charge transport.

3.2 Fourier Transform Infrared (FTIR) Spectroscopy

FTIR spectra were used to confirm chemical bonding and interactions between GO and SCN. Pristine SCN exhibited characteristic bands between 1200–1650 cm^{-1} assigned to stretching vibrations of aromatic C–N and C = N bonds in the triazine rings, and a peak at ~ 810 cm^{-1} corresponding to the breathing mode of the triazine units.

GO showed peaks associated with oxygen-containing functional groups: ~3420 cm^{-1} (O–H stretching), ~ 1720 cm^{-1} (C = O stretching), ~ 1620 cm^{-1} (C = C stretching), and ~ 1220 cm^{-1} (epoxy C–O). In the GO/SCN nanocomposite, characteristic peaks of both SCN and GO

were observed, with slight shifts in band positions, suggesting strong interactions between the GO sheets and SCN matrix. These interactions are expected to facilitate efficient electron transfer during photocatalysis.

3.3 Scanning Electron Microscopy (SEM)

SEM micrographs revealed the morphological features of the materials. SCN exhibited a layered, irregular sheet-like morphology with rough surfaces, typical of graphitic carbon nitride. GO appeared as thin, wrinkled sheets with a folded structure, indicative of its high surface area.

In the GO/SCN nanocomposite, GO sheets were uniformly distributed within the SCN layers, forming an interconnected network. This morphology increases the exposed surface area, provides additional active sites for photocatalytic reactions, and ensures intimate contact between SCN and GO for efficient electron transport. The combination of SCN layers and conductive GO sheets is critical for enhancing photocatalytic performance.

3.4 UV–Visible Diffuse Reflectance Spectroscopy (UV–Vis DRS)

The optical properties of graphene oxide (GO), sulfur carbon nitride (SCN), and the GO/SCN nanocomposite were evaluated using UV–Vis diffuse reflectance spectroscopy (DRS) in the wavelength range of 200–800 nm. The UV–Vis DRS spectra of the materials are presented in Fig. 4. Pristine SCN exhibited a strong absorption edge at approximately 455 nm, indicating its ability to harness visible-light irradiation. In contrast, GO showed weak absorption in the visible region due to its limited light-harvesting capability. Upon incorporation of GO into SCN, the GO/SCN nanocomposite displayed a red shift in the absorption edge to around 475 nm, demonstrating enhanced visible-light absorption resulting from electronic interactions between SCN and GO. The broadening and slight increase in absorption intensity suggest improved light-harvesting efficiency and the potential for higher photocatalytic activity under visible-light irradiation. The optical band gap energies of SCN and the GO/SCN nanocomposite were estimated using Tauc plot analysis for indirect allowed transitions. The Tauc plots are shown in Fig. 5, where $\left(\alpha\, h\nu\right)^{1/2}$ is plotted against photon energy (hv). Extrapolation of the linear region of each curve to the photon energy axis yielded band gap values of 2.72 eV for SCN and 2.58 eV for the GO/SCN nanocomposite. The reduction in band gap for the composite material indicates that the incorporation of GO facilitates more efficient excitation of electrons from the valence band to the conduction band under visible light. This effect enhances the generation of photogenerated electron–hole pairs, thereby improving photocatalytic efficiency. Overall, the UV–Vis DRS and Tauc plot analyses confirm that the GO/SCN heterostructure not only broadens the visible-light absorption range but also narrows the band gap, which are critical factors for the observed enhanced photocatalytic performance.

3.5 BET Surface Area Analysis

BET analysis showed that the GO/SCN nanocomposite possessed a higher specific surface area (68.4 m²/g) compared with pristine SCN (42.7 m²/g).

Figure 6. Nitrogen adsorption–desorption isotherms of the GO/SCN nanocomposite obtained from BET surface area analysis

Nitrogen adsorption–desorption isotherms indicated a mesoporous structure with increased pore volume for the nanocomposite. The enhanced surface area improves adsorption of methylene blue molecules, providing more active sites for photocatalytic reactions and facilitating interaction between the dye molecules and reactive oxygen species.

3.6 Photocatalytic Degradation of Methylene Blue

The photocatalytic performance of the materials was evaluated by monitoring MB degradation under visible-light irradiation.

The GO/SCN nanocomposite exhibited a maximum degradation efficiency of 96.4% within 100 minutes, significantly higher than that of pristine SCN (~ 72%) and GO (~ 15%), demonstrating the synergistic effect of the heterostructure. The improved activity is attributed to: Enhanced visible-light absorption due to band gap narrowing, efficient separation and transport of photogenerated electrons from SCN to GO sheets and increased adsorption of MB molecules on GO surfaces via π–π interactions.

3.7 Kinetic Analysis

The kinetics of methylene blue (MB) degradation were evaluated using the pseudo-first-order kinetic model, which is commonly applied for photocatalytic degradation of organic dyes at low concentrations. The kinetic behavior can be expressed by the following equation:

$$\ln\left(\frac{C_0}{C_t}\right) = kt$$ .....Eq. 3

where C_0 represents the initial concentration of methylene blue, C_t is the concentration at irradiation time *t*, and k is the apparent pseudo-first-order reaction rate constant (min^{-1}). The linear relationship between $\ln(C_0/C_t)$ and irradiation time indicates that the degradation process follows pseudo-first-order kinetics. The kinetic plots derived from the experimental data are presented in Fig. 7. The linearity of these plots demonstrates a strong correlation with the Langmuir–Hinshelwood kinetic model typically observed in heterogeneous photocatalytic reactions. The calculated rate constant (k) for the GO/SCN nanocomposite was 0.032 min^{-1}, which is significantly higher than that obtained for pristine SCN (0.018 min^{-1}) and GO (0.004 min^{-1}). The higher rate constant clearly indicates that the GO/SCN composite exhibits superior photocatalytic activity compared to the individual components.

The enhanced kinetic performance can be attributed to the synergistic interaction between graphene oxide and sulfur carbon nitride, which facilitates rapid charge carrier separation and efficient electron transport. In the GO/SCN system, photogenerated electrons from the conduction band of SCN are effectively transferred to the graphene oxide sheets, which act as electron acceptors and conductive pathways. This electron migration suppresses the recombination of electron–hole pairs, thereby increasing the availability of reactive species such as superoxide radicals ($\bullet O_2^-$) and hydroxyl radicals (•OH) responsible for dye degradation. Furthermore, the increased surface area and mesoporous structure of the GO/SCN nanocomposite enhance adsorption of methylene blue molecules on the catalyst surface, allowing greater interaction with the generated reactive oxygen species. These combined effects contribute to the accelerated degradation kinetics observed for the GO/SCN photocatalyst.

3.8 Radical Scavenger Experiments

To elucidate the mechanism of MB degradation, radical scavenger experiments were performed. The addition of benzoquinone (superoxide radical scavenger) significantly reduced degradation efficiency, indicating that $\bullet O_2^-$ radicals play a major role. Isopropanol (hydroxyl radical scavenger) also suppressed degradation, confirming the involvement of •OH radicals. The presence of EDTA (hole scavenger) slightly decreased degradation efficiency, suggesting that photogenerated holes (h^+) also participate in the oxidation process. These results demonstrate that MB degradation involves multiple reactive species generated by the GO/SCN photocatalyst.

3.9 Catalyst Reusability and Stability

The long-term stability of the GO/SCN nanocomposite was assessed over five consecutive cycles. The degradation efficiencies for cycles 1–5 were: 96.4%, 94.8%, 93.6%, 92.1%, and 90.7%, respectively. The minor decrease is attributed to slight catalyst loss and partial blockage of active sites by intermediates. XRD patterns of the recovered catalyst showed no significant changes, indicating that the crystalline structure of the nanocomposite remained intact after repeated use. These results highlight the excellent photochemical stability and reusability of the GO/SCN photocatalyst for practical wastewater treatment applications.

3.10 Discussion of Synergistic Effects

The enhanced photocatalytic performance of the GO/SCN nanocomposite arises from the synergistic interaction between SCN and GO. Photogenerated electrons from SCN conduction band rapidly transfer to GO sheets, suppressing electron–hole recombination. GO provides additional adsorption sites for MB molecules and enhances light absorption in the visible range. The combined effects of band gap narrowing, efficient charge separation, and improved surface adsorption account for the superior degradation performance and kinetic behavior observed.

5. Conclusion

In this study, a graphene oxide/sulfur carbon nitride (GO/SCN) nanocomposite was successfully synthesized and evaluated as a visible-light-responsive photocatalyst for the degradation of methylene blue (MB) in aqueous solution. The incorporation of GO into SCN significantly enhanced photocatalytic activity by: Improving charge separation and electron mobility through effective electron transfer from SCN to conductive GO sheets, suppressing electron–hole recombination, increasing visible-light absorption, as evidenced by a band gap reduction from 2.72 eV (SCN) to 2.58 eV (GO/SCN) and enhancing adsorption of dye molecules due to the large surface area and π–π interactions provided by GO. The GO/SCN nanocomposite achieved a maximum MB degradation efficiency of 96.4% within 100 min, following pseudo-first-order kinetics (k = 0.032 min^{-1}). Radical scavenger experiments confirmed that superoxide ($\bullet O_2^-$) and hydroxyl (•OH) radicals were the primary reactive species involved, supported by participation of photogenerated holes. Furthermore, the catalyst demonstrated excellent stability and reusability, maintaining > 90% degradation efficiency over five consecutive cycles, with no observable structural degradation. These findings indicate that GO/SCN nanocomposites represent a promising class of metal-free,

visible-light-active photocatalysts for sustainable environmental remediation and wastewater treatment applications. The synergistic heterostructure design offers an effective strategy for improving photocatalytic performance of carbon nitride–based systems.

References

1. Ahmed M, Razu, and Yuta Nishina (2026) Carbon-Based Photocatalysis in Organic Transformation. Bull Chem Soc Jpn : uoaf123
2. Al-Wasidi AS, Ashraf A, Mohamed SA, Mahmoud HA, Ahmed A, Toghan MA, Ahmed, Ahmed MA (2025) PVP-Mediated Graphene Oxide Integration in g-C3N4/NiO Heterojunctions for Enhanced Photocatalytic Tetracycline Degradation. Diam Relat Mater 158:112708
3. Ameen S, Fatima R, Kadhem AA, Abbas T, Khan MA, Abbas A, Hussain I et al (2025) Enhanced Photocatalytic Degradation of Methylene Blue Using Aluminum and Cerium Co-Doped ZnO Nanocomposite. Int J Environ Sci Technol 22(16):16549–16558. 10.1007/s13762-025-06683-z
4. Ayu D, Gusti S, Gea, Andriayani DJ, Telaumbanua Averroes Fazlur Rahman Piliang, Mahyuni Harahap, Zhihao Yen, Ronn Goei, and Alfred Iing Yoong Tok. 2023. Photocatalytic Degradation of Methylene Blue Using N-Doped ZnO/Carbon Dot (N-ZnO/CD) Nanocomposites Derived from Organic Soybean. ACS Omega 8(17): 14965–14984. 10.1021/acsomega.2c07546
5. Dhayal M, Sharma S, Jakhar P, Sain Y, and Himanshu Sharma (2026) Comments Inorg Chem 46(1):30–84. 10.1080/02603594.2025.2494273. Carbon-Supported Photocatalysts: A Sustainable Approach for Enhanced Environmental Remediation.
6. Eswaran P, Madasamy PD, Pillay K, and Hendrik Brink (2025) Sunlight-Driven Photocatalytic Degradation of Methylene Blue Using ZnO/Biochar Nanocomposite Derived from Banana Peels. Biomass Convers Biorefinery 15(8):12347–12367. 10.1007/s13399-024-05999-z
7. Kallawar GA, Bhanvase BA (2023) A Review on Existing and Emerging Approaches for Textile Wastewater Treatments: Challenges and Future Perspectives. Environ Sci Pollut Res 31(2):1748–1789. 10.1007/s11356-023-31175-3
8. Karthik AS, Agrawal S, Senthil S, Debnath A, Devanesan S, Zohier AEA, Vignesh S (2024) One-Pot Synthesis of g-C3N4/N-Doped CeO2 Nanocomposites and Their Potential Visible Light-Driven Photocatalytic Degradation of Methylene Blue Dye. Environ Geochem Health 46(7):246. 10.1007/s10653-024-02007-1
9. Khan W, Ullah S, Ahmed Y, Dhoble, Madhav S (2023) A Critical Review of Hazardous Waste Generation from Textile Industries and Associated Ecological Impacts. J Indian Chem Soc 100(1):100829
10. Kumari S, Singh R, Jahangeer J, and Manoj Chandra Garg (2024) Innovative Strategies for Dye Removal from Textile Wastewater: A Comprehensive Review of Treatment Approaches and Challenges. Water Air Soil Pollut 235(11):720. 10.1007/s11270-024-07532-4
11. Maghanga JK, Osemba M, Ojwang L (2026) Anodic Oxidation of Azo Dyes Using Boron Doped Diamond Electrodes and Silver Nanoparticles. https://scholar.google.com/scholar?cluster=4494650964460281812&hl=en&oi=scholarr (March 5
12. Misra V, Singh V, Singh A, Kumar D, Sharma SK (2023) Photocatalytic Degradation of Methylene Blue Dye in Aqueous Solution under UV Irradiation Using NdMnO3: rGO Hybrid Nanocomposites as a Photocatalyst. Appl Surf Sci Adv 18:100491
13. Mousavi K, Kowsari E, Ramakrishna S, Chinnappan A, Gheibi M (2024) A Comprehensive Review of Greenwashing in the Textile Industry (Life Cycle Assessment, Life Cycle Cost, and Eco-Labeling). Environment, Development and Sustainability 27(9): 21737–77. 10.1007/s10668-024-04508-6
14. Mutuku D, Osemba MO, Thoruwa T, Keheze F (2025) Effect of Chitosan Coating on the Efficiency and Degradation of Solar Panels. Mount Kenya University. https://www.academia.edu/download/128364799/Chitosan_coating.pdf (March 3, 2026)
15. Osemba MO, Muriuki-Hutchins M, Karenga S, Keru G (2024) Production of Chitosan from Crab Shells. Int J Adv Res 7(1):244–250
16. Osemba M, Maghanga J (2025) and Loice Ojwang. Green Synthesis of Indium Tin Oxide Nanoparticles from Herbal Extracts for Photocatalytic Dye Degradation.https://www.researchgate.net/profile/Martin-Osemba/publication/399824967_Green_Synthesis_of_Indium_Tin_Oxide_Nanoparticles_from_Herbal_Extracts_for_Photocatalytic_Dye_Degradation/links/696a08c5abecff2489ec1de0/Green-Synthesis-of-Indium-Tin-Oxide-Nanoparticles-from-Herbal-Extracts-for-Photocatalytic-Dye-Degradation.pdf (March 3, 2026)
17. Osemba MARTINOUMA (2019) Electrochemical Degradation and Chemical Assessment of Azo Dyes in the Textile Waste Water. PhD Thesis. PhD Thesis, Pwani University]. https://elibrary.pu.ac.ke/handle/123456789/826. https://www.researchgate.net/profile/Martin-Osemba/publication/395242671_ELECTROCHEMICAL_DEGRADATION_AND_CHEMICAL_ASSESSMENT_OF_

AZO_DYES_IN_THE_TEXTILE_WASTE_WATER_MARTIN_OUMA_OSEMBA/links/68b8f078360112563e103c4b/ELECTROCHEMICAL-DEGRADATION-AND-CHEMICAL-ASSESSMENT-OF-AZO-DYES-IN-THE-TEXTILE-WASTE-WATER-MARTIN-OUMA-OSEMBA.pdf (March 3, 2026)

18. Veedu SN, Jose S, Narendranath SB, Maliyeckal R, Prathapachandra Kurup, and Pradeepan Periyat (2021) Visible Light-Driven Photocatalytic Degradation of Methylene Blue Dye over Bismuth-Doped Cerium Oxide Mesoporous Nanoparticles. Environ Sci Pollut Res 28(4):4147–4155. 10.1007/s11356-020-10750-y
19. Xie F, Huang C, Dong G, Wu M, Meng D, Yang H, Zhang B, Li Y, and Mingdeng Wei (2025) Sulfur-Doped Carbon Nitride/TiO2 Electron Transport Layer via Glass-Assisted Annealing for High-Efficiency Perovskite Solar Cells. Electrochim Acta : 147804
20. Zhang F, Liu J, Liang H, Guo C (2024) Recent Progress of Three-Dimensional Graphene-Based Composites for Photocatalysis. Gels 10(10):626
21. Zhang J, Wang X, Wang X, Li C (2025) Heterophase Junction Effect on Photogenerated Charge Separation in Photocatalysis and Photoelectrocatalysis. Acc Chem Res 58(6):787–798. 10.1021/acs.accounts.4c00582

Figures

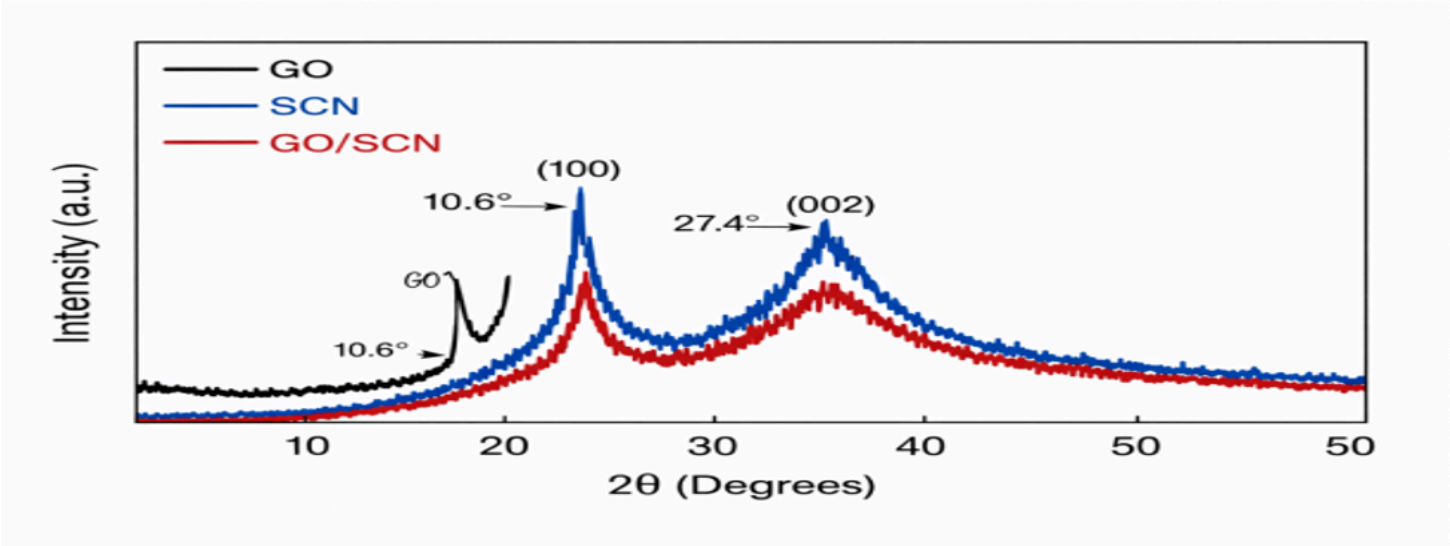


Figure 1

XRD patterns of GO, SCN, and GO/SCN nanocomposite showing characteristic peaks and peak broadening after GO incorporation.

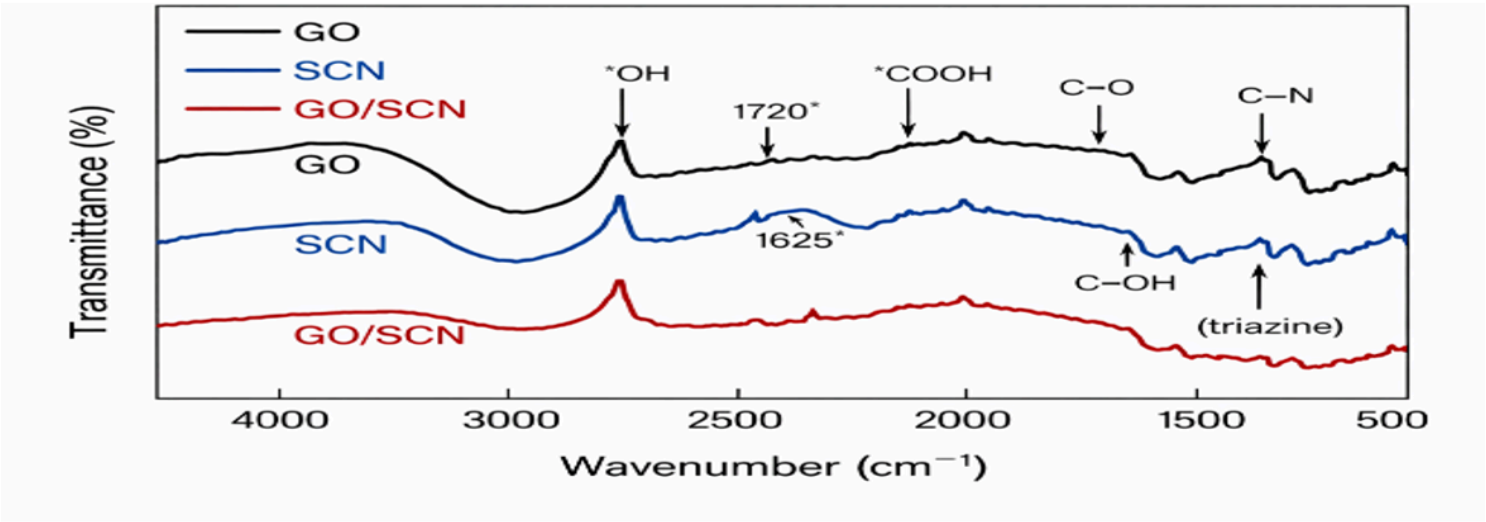


Figure 2

FTIR spectra of GO, SCN, and GO/SCN nanocomposite highlighting characteristic functional groups and peak shifts after GO incorporation.

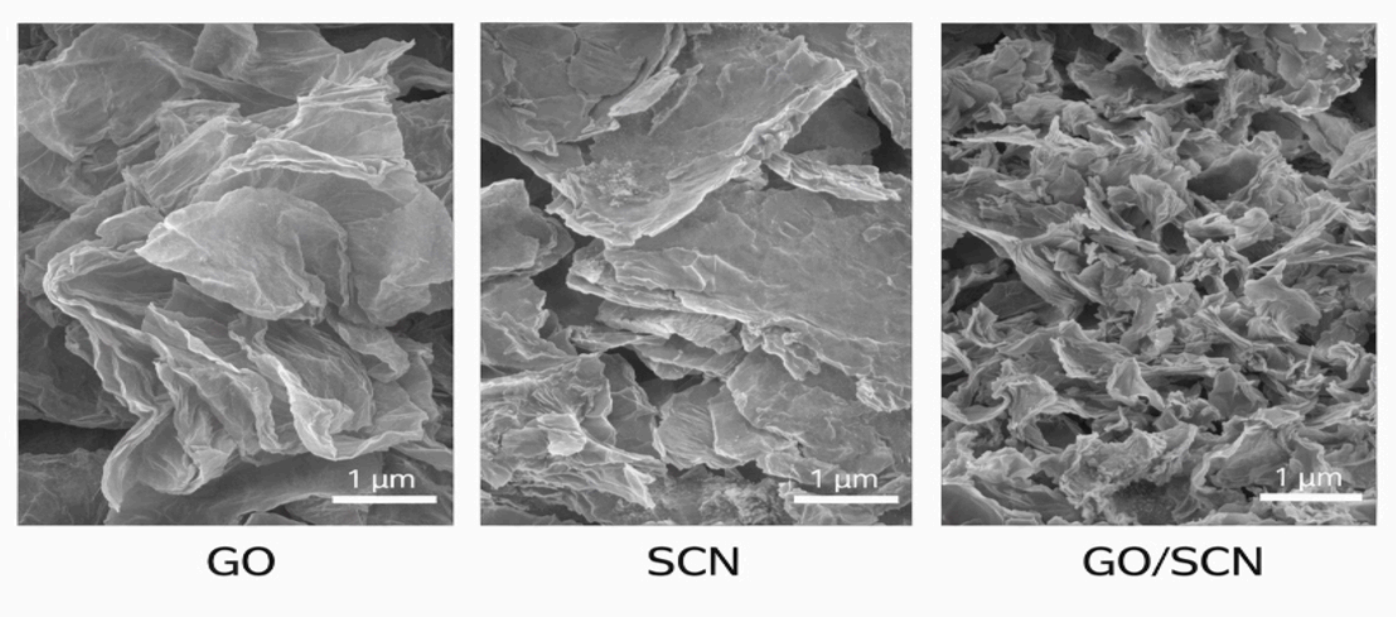


Figure 3

SEM micrographs of GO, SCN, and GO/SCN nanocomposite highlighting layered structures, porous morphology, and combined features after GO incorporation.

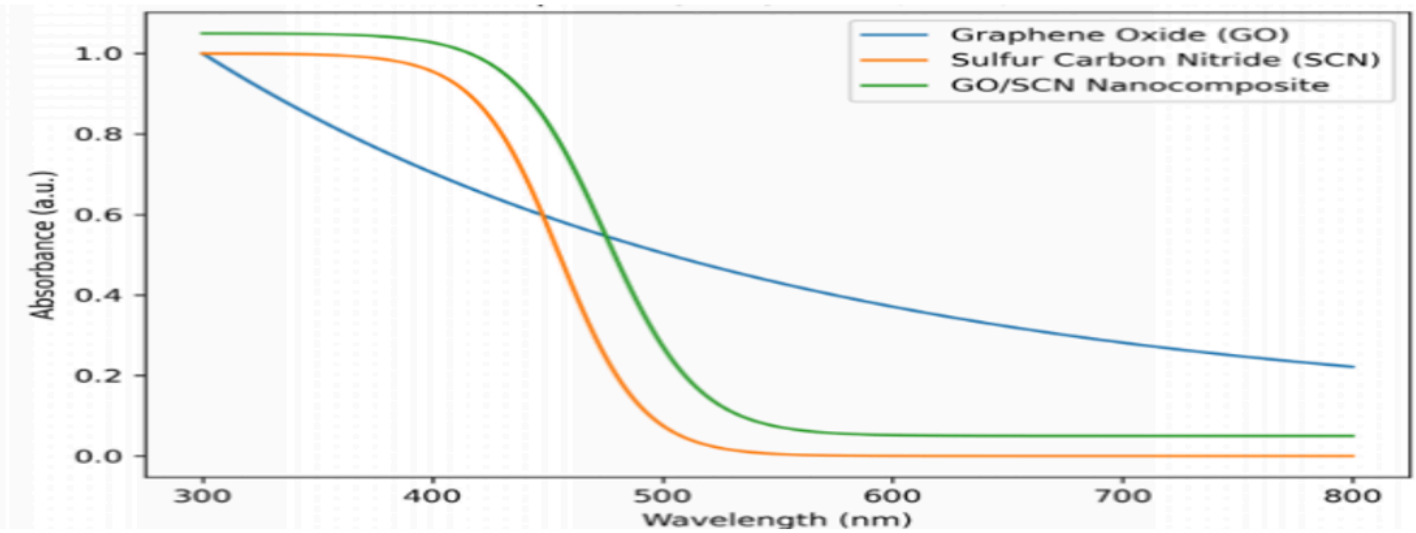


Figure 4

UV–Vis diffuse reflectance spectra of graphene oxide (GO), sulfur carbon nitride (SCN), and the GO/SCN nanocomposite.

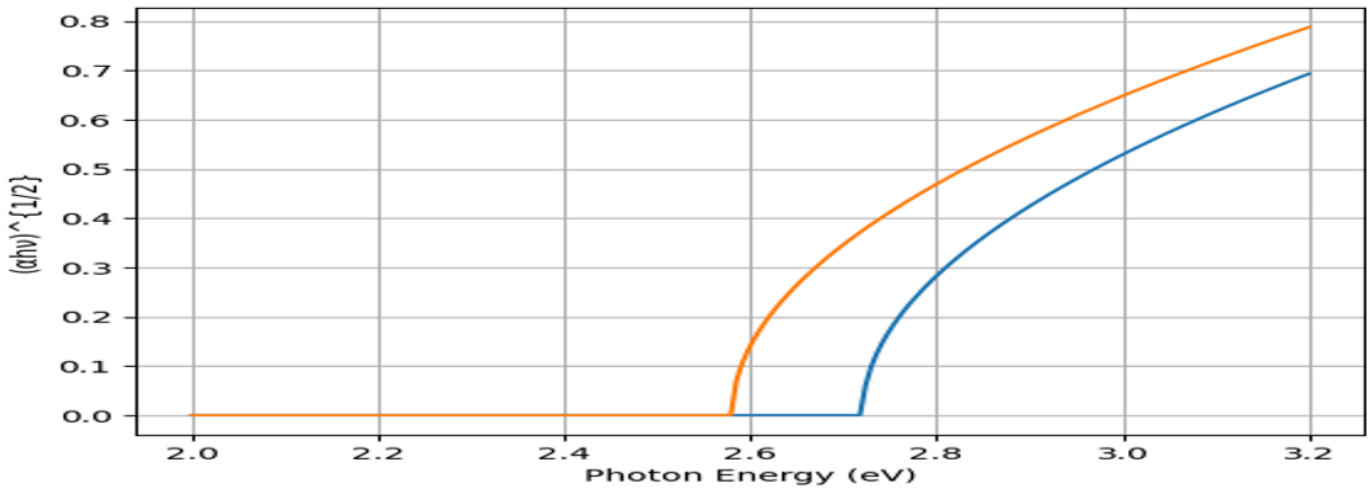


Figure 5

Tauc plots $(\alpha h\nu)^{1/2}$ *versus photon energy (hv) for SCN and the GO/SCN nanocomposite, used to estimate optical band gap energies*

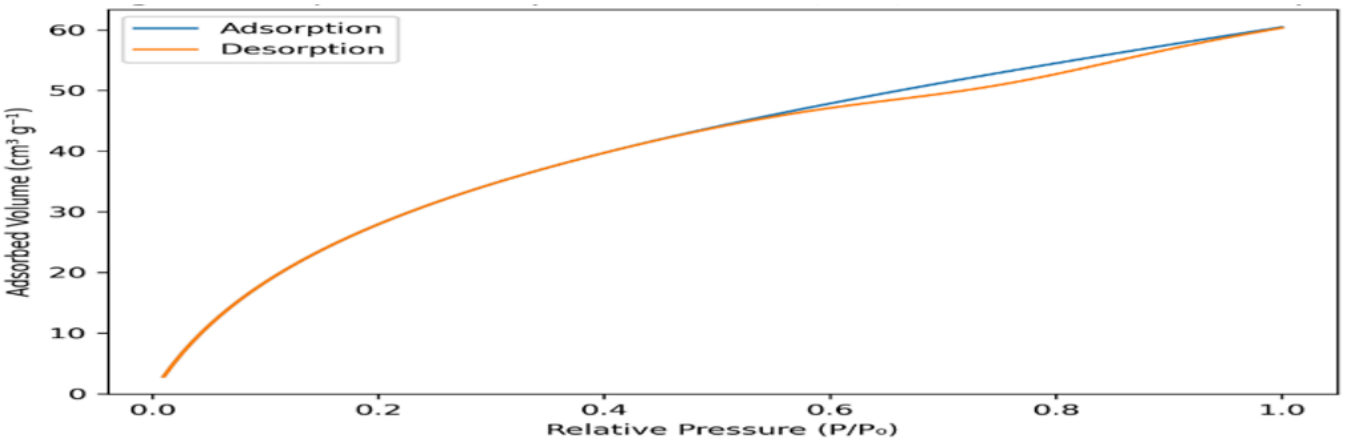


Figure 6

Nitrogen adsorption–desorption isotherms of the GO/SCN nanocomposite obtained from BET surface area analysis

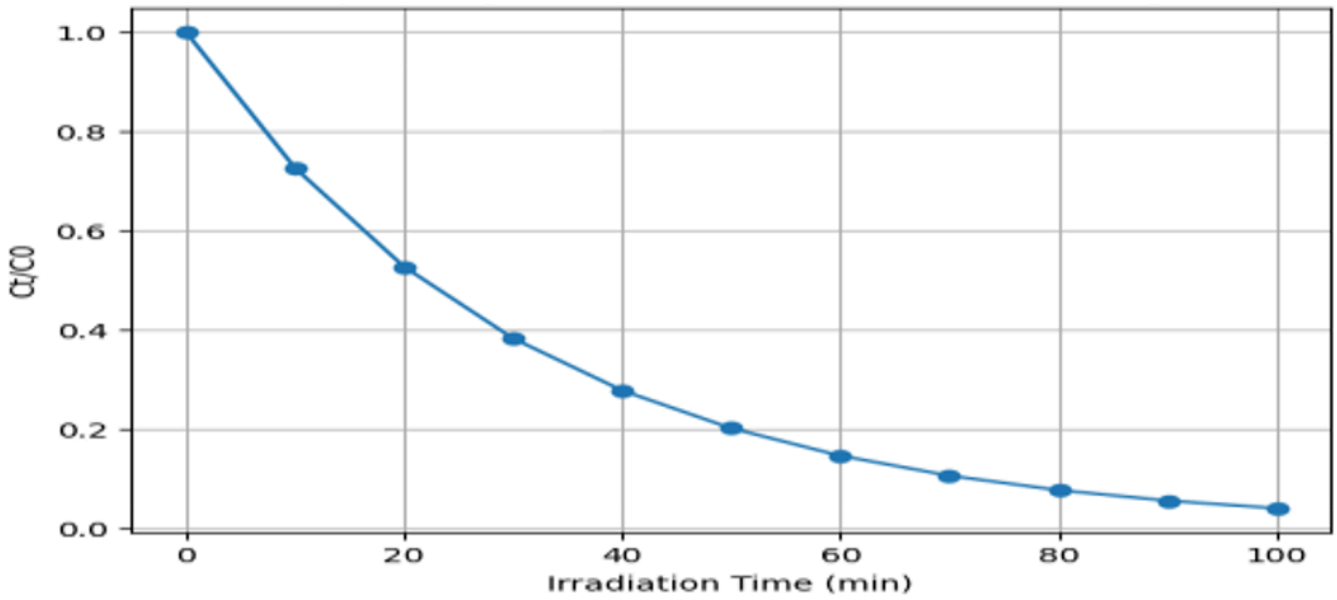


Figure 7

Photocatalytic degradation profile of methylene blue (MB) under visible-light irradiation using the GO/SCN nanocomposite.

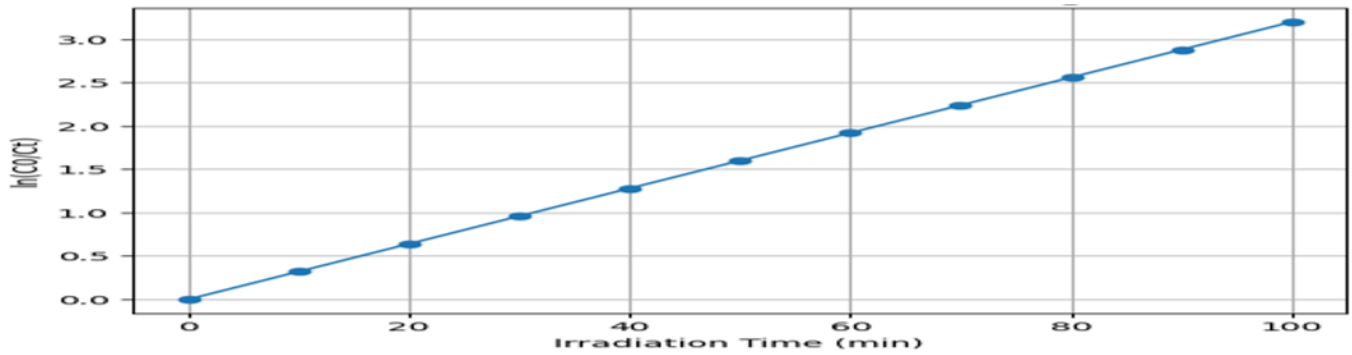


Figure 8

Pseudo-first-order kinetic analysis of methylene blue degradation using the GO/SCN photocatalyst.